nature geoscience

LETTERS

PUBLISHED ONLINE: 27 APRIL 2015 | DOI: 10.1038/NGEO2422

Links between atmospheric carbon dioxide, the land carbon reservoir and climate over the past millennium

Thomas K. Bauska[1]*, Fortunat Joos[2], Alan C. Mix[1], Raphael Roth[2], Jinho Ahn[3] and Edward J. Brook[1]

The stability of terrestrial carbon reservoirs is thought to be closely linked to variations in climate[1], but the magnitude of carbon–climate feedbacks has proved difficult to constrain for both modern[2–4] and millennial[5–13] timescales. Reconstructions of atmospheric CO_2 concentrations for the past thousand years have shown fluctuations on multidecadal to centennial timescales[5–7], but the causes of these fluctuations are unclear. Here we report high-resolution carbon isotope measurements of CO_2 trapped within the ice of the West Antarctic Ice Sheet Divide ice core for the past 1,000 years. We use a deconvolution approach[14] to show that changes in terrestrial organic carbon stores best explain the observed multidecadal variations in the $\delta^{13}C$ of CO_2 and in CO_2 concentrations from 755 to 1850 CE. If significant long-term carbon emissions came from pre-industrial anthropogenic land-use changes over this interval, the emissions must have been offset by a natural terrestrial sink for ^{13}C-depleted carbon, such as peatlands. We find that on multidecadal timescales, carbon cycle changes seem to vary with reconstructed regional climate changes. We conclude that climate variability could be an important control of fluctuations in land carbon storage on these timescales.

Atmospheric $\delta^{13}C$-CO_2 reflects the integrated impact of land and ocean carbon sources and sinks. Exchange among these reservoirs modifies the relative proportions of carbon isotopes in the atmosphere, allowing some sources and sinks of CO_2 to be differentiated. During photosynthesis, ^{12}C is preferentially taken up relative to ^{13}C into organic carbon reservoirs. When more organic carbon is stored on land or exported to the deep ocean, atmospheric CO_2 decreases and becomes more enriched in ^{13}C ($\delta^{13}C$-CO_2 increases), yielding a negative correlation between atmospheric CO_2 concentration and $\delta^{13}C$-CO_2. Conversely, CO_2 outgassing from dissolved inorganic carbon in response to sea surface warming is associated with a decrease in the magnitude of fractionation during air–sea gas exchange, yielding a positive correlation between atmospheric CO_2 and $\delta^{13}C$-CO_2. Changes in the marine cycle of calcium carbonate or the volcanic input of CO_2 to the atmosphere have a small effect on $\delta^{13}C$-CO_2.

We constructed a new precise record of $\delta^{13}C$-CO_2 and extended a previous high-resolution CO_2 record[8] using samples from the Antarctic WAIS Divide Ice Core (West Antarctic Ice Sheet, 79.467° S, 112.085° W, ice elevation 1,769 m). Our reconstruction spans the interval 755–1915 CE with decadal resolution. The precisions of $\delta^{13}C$-CO_2 and CO_2 measurements are ±0.016‰ and 0.8 ppm, respectively, and the $\delta^{13}C$-CO_2 record is accurate to within about ±0.04‰ of the NOAA and NBS reference scheme[15].

Our record reveals relatively stable atmospheric CO_2 and $\delta^{13}C$-CO_2 between 755 and 950 CE (Fig. 1). Between 975 and 1080 CE atmospheric CO_2 increased by 5 ppm and $\delta^{13}C$-CO_2 decreased by 0.08‰. Atmospheric CO_2 then slowly decreased, and $\delta^{13}C$-CO_2 slowly increased until about 1370 CE. At that time atmospheric CO_2 began to decrease more quickly and $\delta^{13}C$-CO_2 started to increase, but this trend quickly reversed around 1440 CE, followed by a rapid 3–4 ppm CO_2 increase and a 0.1‰ $\delta^{13}C$-CO_2 decrease between 1475–1490 CE. The most prominent change before 1850 CE occurred from 1530–1620 CE, when $\delta^{13}C$-CO_2 increased by 0.2‰ and CO_2 decreased by 6 ppm. After 1700 CE, $\delta^{13}C$-CO_2 decreased and CO_2 increased, with a significant increase in rates of change at the onset of the industrial period (~1850 CE).

Much of the variability exhibited in our record was not resolved in the previous attempts to reconstruct atmospheric $\delta^{13}C$-CO_2 over the past millennium (Fig. 1). Well-resolved surface-ocean $\delta^{13}C$ variations post-1400 CE in Caribbean corals[16] (25 m depth), however, are consistent with our data (Fig. 1) and support the reliability of our record as a high-fidelity record of the atmosphere. The near constant isotopic offset of about 0.08‰ between the lower-resolution Law Dome record and this study is possibly due to different reference schemes used at CSIRO and OSU (see Supplementary Information).

Increasing CO_2 concentration is associated with decreasing $\delta^{13}C$-CO_2 between 755 and 1850 CE ($R^2 = 0.54$; Fig. 1 inset). This negative slope rules out ocean temperature changes as the main driver of atmospheric CO_2 variability in this time interval and is consistent with variations in a ^{13}C-depleted organic carbon reservoir, most likely the land biosphere, as the primary control on atmospheric CO_2 variability. However, we cannot rule out from the atmospheric data alone that changes in ocean circulation, the efficiency of the ocean's biological pump or air–sea gas exchange contributed to a portion of the $\delta^{13}C$-CO_2 variability, particularly on the millennial timescale. Nor can the data delineate changes in the photosynthetic pathway (that is, C3/C4 abundance) that may change the net carbon isotopic discrimination within plants and must be treated as uncertainty (see below).

We used a well-established 'double-deconvolution' technique to derive a suite of land–atmosphere and ocean–atmosphere flux histories from the HILDA box model[14] with a range of scenarios for the evolution of sea surface temperature (SST) from an annually resolved global temperature reconstruction[17]. Deconvolving the atmospheric CO_2 and $\delta^{13}C$ budgets reveals plausible multidecadal-scale organic land carbon variability. Organic land carbon decreases by 20 GtC from 950–1100 CE and increases by 50 GtC

[1]College of Earth, Ocean, and Atmospheric Sciences, Oregon State University, Corvallis, Oregon 97331, USA. [2]Climate and Environmental Physics, Physics Institute and Oeschger Center for Climate Change Research, University of Bern, CH-3012 Bern, Switzerland. [3]School of Earth and Environmental Science, Seoul National University, Seoul 151-742, Korea. *e-mail: bauskat@geo.oregonstate.edu

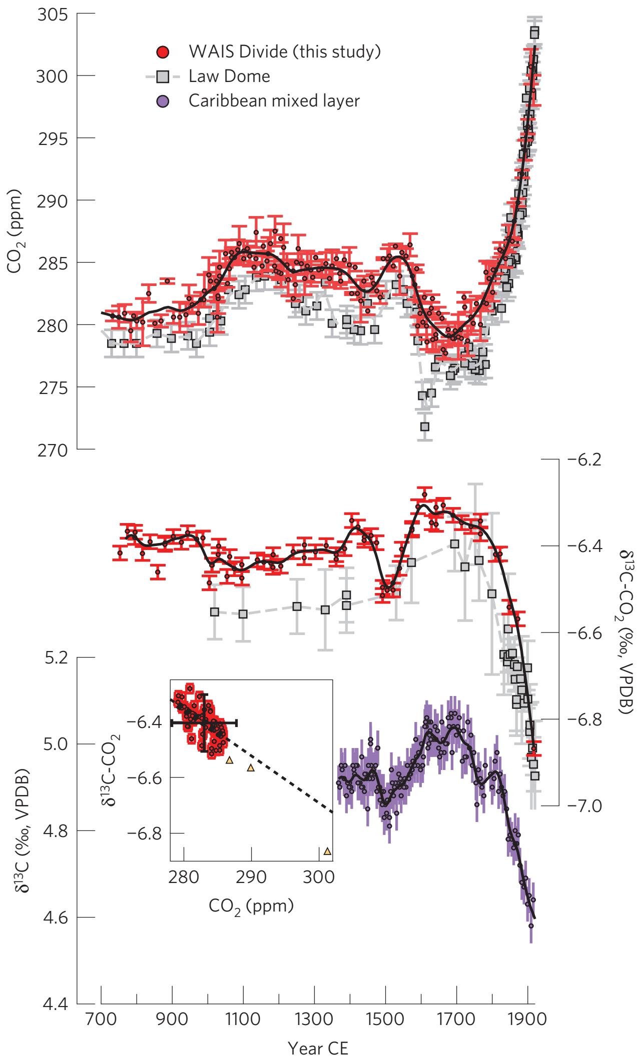

Figure 1 | Carbon cycle variability of the past millennium. CO_2 and $\delta^{13}C$-CO_2 (red markers, this study) from the WAIS Divide Ice Core with earlier reconstructions from the Law Dome ice core (grey markers)[6,11] and a pristine coral $\delta^{13}C$ record[16] (purple markers) from the near-surface Caribbean (25 m water depth, 78° 57′ W, 17° 32′ N). Errors bars show the estimated uncertainty at the 1-σ s.d. level. Inset is a cross plot of the WAIS Divide CO_2 and $\delta^{13}C$-CO_2 data for the pre-industrial (~755—1850 CE; red circles with the mean and 2-σ standard deviation indicated by black error bars and linear fit with a dashed black line) as well as the data covering the industrial period (~1850–1915 CE; yellow triangles).

from 1200–1750 CE, superimposed on a longer-term increase of about 30 GtC ka^{-1} between 755–1850 CE (Fig. 2a). The impact of random uncertainties is evaluated by running Monte Carlo simulations ($n = 1{,}000$) in which the data input (CO_2, $\delta^{13}C$-CO_2, SST) and the globally averaged photosynthetic fractionation factor (ε-photo $= -18 \pm 2$‰) were varied within their estimated error. The following experiments were carried out to constrain systematic error: we used a largely independent reconstruction of global temperature[18] with lower temporal resolution but better spatial coverage in the oceanic basins to prescribe SST and separately imposed secular and high-frequency variability in the photosynthetic fractionation factor (see Supplementary Information). The multidecadal variations are insensitive to these potential errors, but the millennial-scale trend in organic land carbon gained could range between 0 and +50 GtC ka^{-1} if long-term trends in the photosynthetic fractionation factor of 0.2‰ ka^{-1} are considered. The data therefore probably rule out a decrease in net stocks of organic land carbon between 755 and 1850 CE.

Our estimates of land carbon variability based on double-deconvolution of the CO_2 and $\delta^{13}C$ data help to constrain mechanisms that influenced the pre-industrial carbon cycle. A gradual re-growth of peatland throughout the Holocene epoch, as a long-term response to the last deglaciation, is thought to be a significant sink for atmospheric CO_2. For the past millennium, estimates range between about ~+30–50 GtC ka^{-1} (ref. 19) with minor multidecadal-scale variability recorded in the carbon accumulation[20]. Expansion of human population can drive land conversion and has been suggested to decrease land carbon stocks with a significant impact on pre-industrial atmospheric CO_2 during the late Holocene[13]. The magnitude of this effect is not well constrained. Estimates vary between about 50 GtC of land carbon loss between ~750 and 1850 CE (overall trend = ~−30 GtC ka^{-1}) in many models[21,22] to about 150 GtC in one model[23] (overall trend = ~−97 GtC ka^{-1}; Fig. 2a). The larger loss of land carbon to the atmosphere from human impacts in the 'KK10' model[23], which implies a significant role for anthropogenic processes on the pre-industrial carbon cycle, are mainly linked to a greater extent of soil carbon depletion after land conversions and higher assumed per capita land use at low population densities as opposed to an assumed linear relationship between population and land use (as in 'HYDE-LPX'; ref. 22). Only land conversion, which can include shifting cultivation, urbanization, land abandonment, harvest on agricultural land, wood harvest, legacy fluxes and the dynamics of soil, vegetation and product pools[24], is at present considered in model-based estimates of anthropogenic emissions. Other possible pre-industrial anthropogenic CO_2 sources such as peatland drainage, peat extraction and peat fires, the early use of fossil fuel resources, as well as possible CO_2 sinks such a rice cultivation, construction of reservoirs, or irrigation are at present too uncertain to obtain quantitative estimates during the pre-industrial period.

Because $\delta^{13}C$-CO_2 reflects the net effect of natural and anthropogenic sources and sinks of CO_2, the impacts of natural processes can be estimated by taking the difference between modelled LUC scenarios and our constraints on net organic land carbon change from the deconvolution (Fig. 2b). The anthropogenic carbon emissions in the HYDE-LPX scenario require partial compensation by carbon uptake through natural processes of about +60 GtC ka^{-1}, similar in magnitude to estimates of the long-term uptake by peatland, with multidecadal-scale changes driven by natural climate–carbon feedbacks. The KK10 scenario requires +124 GtC ka^{-1} of carbon uptake by natural processes, suggesting either a substantially underestimated peatland uptake (~2.5–4 times to low), an extremely sensitive climate–carbon feedback to a small 0.1–0.3 °C ka^{-1} cooling trend over the past millennium[25], and/or a hitherto unidentified land carbon sink. Alternatively, it has recently been suggested that LUC scenarios may not accurately represent the net anthropogenic land carbon flux to the atmosphere, possibly because (like most current carbon cycle models) the burial of eroded organic carbon on hillslopes and floodplains following erosion is neglected[26].

Because the long-term trend in $\delta^{13}C$-CO_2 and organic land carbon uptake seems to require a balance between LUC emissions and peatland uptake, we investigate the role of climate–carbon feedbacks by testing the sensitivity of land carbon to climate on the multidecadal timescale. Moreover, regional climate shows distinctly different patterns at a multidecadal timescale[25] (Fig. 3), offering an opportunity to understand which regions dominate the natural carbon cycle budget. However, this requires us to assume that pre-industrial anthropogenic CO_2 emissions are minor on the multidecadal timescale.

We constructed a simple statistical model of the relationship between our carbon cycle observations and a suite of regional

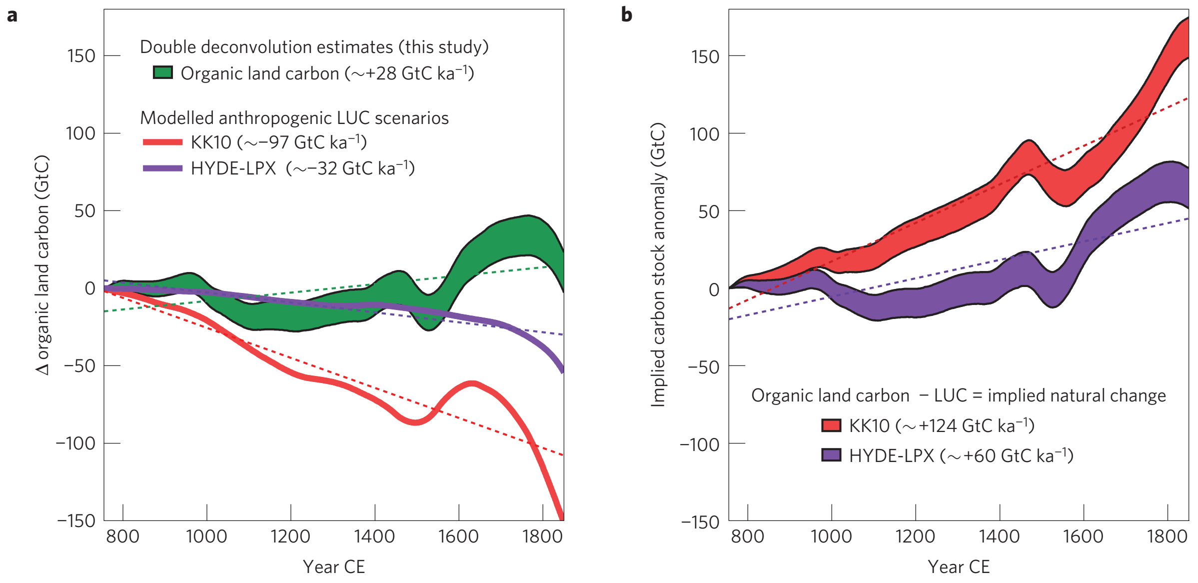

Figure 2 | Double-deconvolution results and anthropogenic emission scenarios. a, Reconstructed changes in organic land carbon with 1-σ standard deviation uncertainty (green shading), modelled anthropogenic land-use change from the KK10 model[23] (red) and HYDE-LPX model[22] (purple). **b**, Difference in total organic land carbon change and anthropogenic emissions implying the natural organic land carbon from the KK10 (red shading) and HYDE-LPX (purple shading) scenarios. Dotted lines indicate linear trends from 755–1850 CE.

Table 1 | Summary of multiple and single linear regression model coefficients at various time constants (τ) with 'NS' indicating nonsignificant results at the 99% confidence interval.

	Multiple linear regression model of regional temperatures							Single linear regression NH temp.	
τ (yr)	Adj. R^2	$\beta \pm$ s.e.m. (GtC K^{-1})						R^2	$\beta \pm$ s.e.m. (GtC K^{-1})
		Arctic	Africa	Asia	N. America	S. America	Europe		
25	0.38	−53 ± 11	−19 ± 7	NS	NS	NS	NS	0.46	−56 ± 10
50	0.56	−74 ± 11	−27 ± 7	NS	NS	NS	NS	0.57	−67 ± 9
75	0.66	−89 ± 10	−33 ± 7	NS	NS	NS	NS	0.65	−77 ± 9
100	0.73	−102 ± 10	−38 ± 7	NS	NS	NS	NS	0.70	−85 ± 9
125	0.77	−113 ± 10	−43 ± 7	NS	NS	NS	NS	0.74	−94 ± 9
150	0.86	−128 ± 18	−62 ± 7	142 ± 32	−135 ± 43	NS	NS	0.77	−102 ± 9

temperature reconstructions before the Industrial Revolution. Briefly, annually resolved regional temperature reconstructions are passed through an exponential response function with a range of e-folding times based on plausible soil carbon residence times[27] (25–150 years) and then entered, if significant at the 99% confidence interval, as independent variables in a multiple linear regression (MLR) model of organic land carbon changes. We also constructed a similar model with a Northern Hemisphere temperature reconstruction[17] as the single independent variable. Our approach is limited to a qualitative description of the climate–carbon feedback, primarily by uncertainties in the temperature reconstructions, but also our inability to describe dynamics related to precipitation, extreme events and hysteresis that process-based models can capture. Negative regression coefficients (β) indicate decreases in organic land carbon with increased temperature (that is, a positive feedback between warming and carbon flux to the atmosphere).

Between carbon response e-folding times of 25–125 years, Arctic temperature may dominate the organic land carbon changes, entering the MLR model first, followed by tropical African temperature. Together, positive climate–carbon feedbacks in the Arctic and Africa can explain about 38–77% of the variance in organic land carbon (Table 1). At larger e-folding timescales, North American and Asian temperature enter the MLR model, but the variance explained increases by less than 10% and multicollinearity of the independent variables in the model increases (Supplementary Table 4), suggesting the result at larger e-folding times should be treated with caution. Alternatively, the regression model suggests that Northern Hemisphere (NH) temperature as a positive feedback can explain similar amounts of variance to the MLR (Table 1).

The Arctic at present holds about 1500 GtC belowground (∼50% of the global total)[28] in some of the longest-lived carbon terrestrial reservoirs[27]. Our illustrative analysis suggests that maxima in Arctic temperature from 950–1050 CE and 1400–1600 CE are associated with decreases in δ^{13}C-CO_2 and organic land carbon. The lagged response is consistent with a source of carbon from a long-lived carbon reservoir such as peatland decay; carbon trapped in permafrost; or boreal forests and soils. Records of NH peatland accumulation have a positive correlation with NH temperature over the past millennium, which had previously suggested a negative (albeit small) feedback between temperature and peatland carbon[20]. Peatlands as the dominant source of CO_2 during Arctic warm intervals would require a mechanism whereby decay of deeper peat layers in response to short-term warming would significantly outpace long-term Holocene accumulation. Permafrost carbon is also a plausible source of CO_2 to the atmosphere during intervals of elevated Arctic temperature, but would require re-expansion

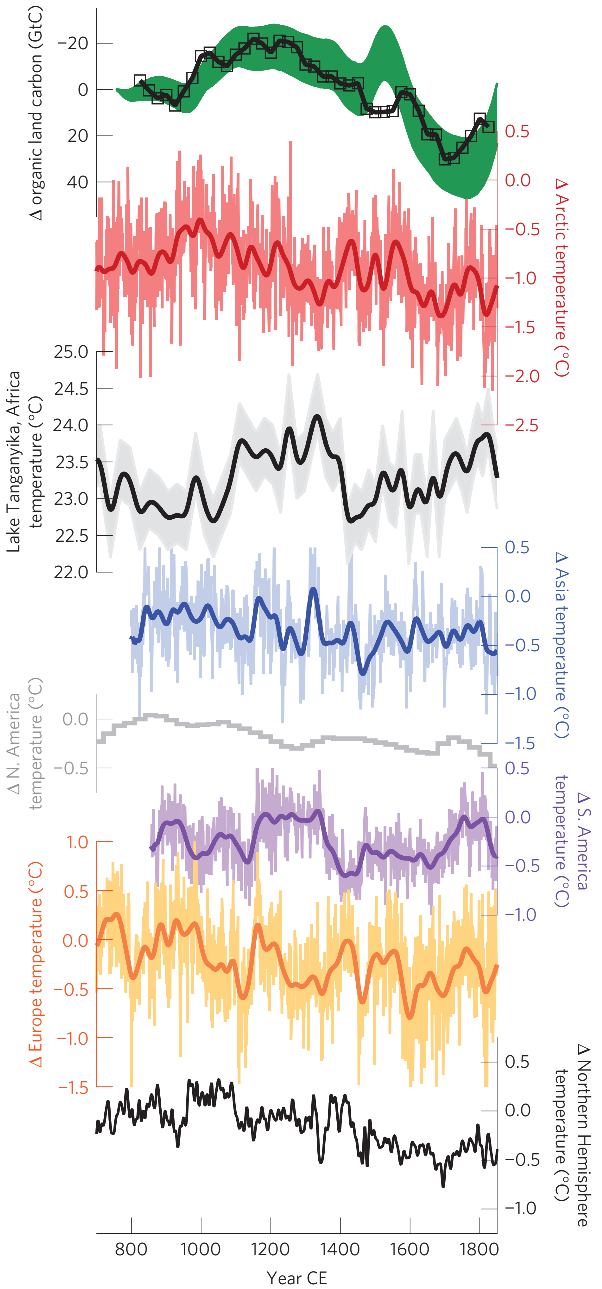

Figure 3 | Multidecadal climate and carbon cycle variability. Reconstructed change in organic land carbon stocks (green shading) with the MLR model prediction at the 100-year time constant (black markers). Land carbon changes are plotted on a inverted axis to show possible correlations with regional temperature reconstructions[25] of the Arctic (red), Asia (blue), N. America (grey), S. America (purple), Europe (yellow), Lake Tanganyika temperature[30]—as a plausible representation of tropical Africa (thick black with uncertainty in grey)—and a Northern Hemisphere composite (thin black line).

of permafrost into previously active soils during cold intervals to act as a sink for CO_2. The soil and vegetation of the boreal forest biome, with both production and respiration, is also a candidate for an active reservoir on multidecadal to centennial timescales.

Other regional-scale reconstructions are all negatively, but moderately correlated to $\delta^{13}C$-CO_2 and organic land carbon changes, with only tropical African temperature entering the MLR model after Arctic temperature. Tropical temperature variations thus may have played a role in land carbon storage, but temperature reconstructions for these regions are too imprecise to be certain. For example, a strong cooling around 1350 CE in tropical Africa and South America may have contributed to the overall increase in land carbon from about 1350–1700 CE.

Our statistical model suggests that climate can account for most of the changes in land carbon (Fig. 3), but underestimates decreases in land carbon around 1500 CE and the subsequent increase until about 1700 CE. Land carbon uptake following widespread pandemics in the New World has been suggested as playing a role in this interval, but sensitivity to anthropogenic effects on the multidecadal scale has not been supported by some LUC models[22,29]. After removing the linear trend in KK10 model results from 755–1850 CE (−96 GtC ka^1), this LUC scenario shows common features with our inferred land carbon stocks on the multidecadal timescale ($R^2 = 0.36$), but this model scenario requires a persistent and substantial natural land carbon sink during the past millennium as well as a significant acceleration of land carbon loss around 1700 CE that is not supported by our data.

Our results put strong limits on the net source of land carbon to the atmosphere before the industrial period. The carbon isotope data permit a range of scenarios for anthropogenic carbon releases, but require that anthropogenic releases be offset by an equally large land carbon sink. Although uncertainty remains in regional temperature reconstructions over the past millennium, our finding that temperature changes may plausibly account for most of the reconstructed variations in organic land carbon over the past millennium is consistent with hypothesized release of land carbon during future global climate change; of particular concern may be amplified warming at high northern latitudes.

Methods

Code availability. The code used to generate the land–atmosphere and ocean–atmosphere flux histories is available on request from Fortunat Joos (joos@climate.unibe.ch).

Data. Data are available from http://ncdc.noaa.gov/paleo/study/18316.

Received 27 October 2014; accepted 19 March 2015; published online 27 April 2015

References

1. Ciais, P. *et al.* in *Climate Change 2013: The Physical Science Basis* (eds Stocker, T. F. *et al.*) 465–570 (IPCC, Cambridge University Press, 2013).
2. Trumbore, S. E. & Czimczik, C. I. An uncertain future for soil carbon. *Science* **321,** 1455–1456 (2008).
3. Hopkins, F. M., Torn, M. S. & Trumbore, S. E. Warming accelerates decomposition of decades-old carbon in forest soils. *Proc. Natl Acad. Sci. USA* **109,** 1753–1761 (2012).
4. Arora, V. K. *et al.* Carbon-concentration and carbon–climate feedbacks in CMIP5 Earth System Models. *J. Clim.* **26,** 5289–5314 (2013).
5. Siegenthaler, U. R. S. *et al.* Supporting evidence from the EPICA Dronning Maud Land ice core for atmospheric CO_2 changes during the past millennium. *Tellus B* **57,** 51–57 (2005).
6. MacFarling, C. *et al.* Law Dome CO_2, CH_4 and N_2O ice core records extended to 2000 years BP. *Geophys. Res. Lett.* **33,** L14810 (2006).
7. Ahn, J. *et al.* Atmospheric CO_2 over the last 1000 years: A high-resolution record from the West Antarctic Ice Sheet (WAIS) Divide ice core. *Glob. Biogeochem. Cycles* **26,** GB2027 (2012).
8. Joos, F., Meyer, R., Bruno, M. & Leuenberger, M. The variability in the carbon sinks as reconstructed for the last 1000 years. *Geophys. Res. Lett.* **26,** 1437–1440 (1999).
9. Trudinger, C. M., Enting, I. G., Rayner, P. J. & Francey, R. J. Kalman filter analysis of ice core data—2. Double deconvolution of CO_2 and delta C-13 measurements. *J. Geophys. Res.* **107,** 4423 (2002).
10. Francey, R. J. *et al.* A 1000-year high precision record of $\delta^{13}C$ in atmospheric CO_2. *Tellus B* **51,** 170–193 (1999).
11. Rubino, M. *et al.* A revised 1000-year atmospheric $\delta^{13}C$-CO_2 record from Law Dome and South Pole, Antarctica. *J. Geophys. Res.* **118,** 8482–8499 (2013).

12. Frank, D. C. *et al.* Ensemble reconstruction constraints on the global carbon cycle sensitivity to climate. *Nature* **463,** 527–U143 (2010).
13. Ruddiman, W. F. The anthropogenic greenhouse era began thousands of years ago. *Climatic Change* **61,** 261–293 (2003).
14. Joos, F. & Bruno, M. Long-term variability of the terrestrial and oceanic carbon sinks and the budgets of the carbon isotopes C-13 and C-14. *Glob. Biogeochem. Cycles* **12,** 277–295 (1998).
15. Bauska, T. K., Brook, E. J., Mix, A. C. & Ross, A. High precision dual-inlet IRMS measurements of the stable isotopes of CO_2 and the N_2O/CO_2 ratio from polar ice core samples. *Atmos. Meas. Tech. Discuss.* **7,** 6529–6564 (2014).
16. Böhm, F. *et al.* Evidence for preindustrial variations in the marine surface water carbonate system from coralline sponges. *Geochem. Geophys. Geosyst.* **3,** http://dx.doi.org/10.1029/2001GC000264 (2002).
17. Mann, M. E. *et al.* Proxy-based reconstructions of hemispheric and global surface temperature variations over the past two millennia. *Proc. Natl Acad. Sci. USA* **105,** 13252–13257 (2008).
18. Marcott, S. A., Shakun, J. D., Clark, P. U. & Mix, A. C. A reconstruction of regional and global temperature for the past 11,300 years. *Science* **339,** 1198–1201 (2013).
19. Spahni, R., Joos, F., Stocker, B. D., Steinacher, M. & Yu, Z. C. Transient simulations of the carbon and nitrogen dynamics in northern peatlands: From the Last Glacial Maximum to the 21st century. *Clim. Past* **9,** 1287–1308 (2013).
20. Charman, D. J. *et al.* Climate-related changes in peatland carbon accumulation during the last millennium. *Biogeosciences* **10,** 929–944 (2013).
21. Pongratz, J., Reick, C. H., Raddatz, T. & Claussen, M. Effects of anthropogenic land cover change on the carbon cycle of the last millennium. *Glob. Biogeochem. Cycles* **23,** GB4001 (2009).
22. Stocker, B. D., Strassmann, K. & Joos, F. Sensitivity of Holocene atmospheric CO_2 and the modern carbon budget to early human land use: Analyses with a process-based model. *Biogeosciences* **8,** 69–88 (2011).
23. Kaplan, J. O. *et al.* Holocene carbon emissions as a result of anthropogenic land cover change. *Holocene* **21,** 775–791 (2011).
24. Stocker, B. D., Feissli, F., Strassmann, K. M., Spahni, R. & Joos, F. Past and future carbon fluxes from land use change, shifting cultivation and wood harvest. *Tellus B* **66,** 23188 (2014).
25. PAGES 2k Consortium Continental-scale temperature variability during the past two millennia. *Nature Geosci.* **6,** 339–346 (2013).
26. Hoffmann, T. *et al.* Short Communication: Humans and the missing C-sink: Erosion and burial of soil carbon through time. *Earth Surf. Dynam.* **1,** 45–52 (2013).
27. Carvalhais, N. *et al.* Global covariation of carbon turnover times with climate in terrestrial ecosystems. *Nature* **514,** 213–217 (2014).
28. Tarnocai, C. *et al.* Soil organic carbon pools in the northern circumpolar permafrost region. *Glob. Biogeochem. Cycles* **23,** GB2023 (2009).
29. Pongratz, J., Caldeira, K., Reick, C. H. & Claussen, M. Coupled climate–carbon simulations indicate minor global effects of wars and epidemics on atmospheric CO_2 between ad 800 and 1850. *Holocene* **21,** 843–851 (2011).
30. Tierney, J. E. *et al.* Late-twentieth-century warming in Lake Tanganyika unprecedented since AD 500. *Nature Geosci.* **3,** 422–425 (2010).

Acknowledgements

Carbon isotope work was supported by NSF Grant 0839078 (E.J.B. and A.C.M.). Oregon State University provided additional support for mass spectrometer purchase and management of the OSU/CEOAS stable isotope laboratory. J.A. was partially supported by a National Research Foundation of Korea (NRF) Grant funded by the Korean Government (MSIP) 2014R1A1A2A16054779. F.J. and R.R. are grateful for financial contributions by the Swiss National Science Foundation, including contributions through the Sinergia Project iTree (grant no. 136295), and by the European Commission through the FP7 project CARBOCHANGE (grant no. 264879) and Past4Future (grant no. 243908). We appreciate the support of the WAIS Divide Science Coordination Office for the collection and distribution of the WAIS Divide ice core (Kendrick Taylor (Desert Research Institute of Reno Nevada), NSF Grants 0230396, 0440817, 0944348 and 0944266—University of New Hampshire). The NSF also funds the Ice Drilling Program Office, Ice Drilling Design and Operations group, which leads coring activities, and The National Ice Core Laboratory, which curates the core and performs core processing. We thank J. Severinghaus for providing $\delta^{15}N$ of N_2 data, Raytheon Polar Services for logistics support in Antarctica, and the 109th New York Air National Guard for airlift in Antarctica.

Author contributions

T.K.B., E.J.B. and A.C.M. designed the study with the climate–carbon cycle analysis conceived and performed by T.K.B. and A.C.M. T.K.B. developed the carbon isotope analytical system with E.J.B. and A.C.M. T.K.B. produced the carbon isotope data and J.A. produced the CO_2 concentration data. F.J. and R.R. assisted T.K.B. with the deconvolution modelling. T.K.B. wrote the manuscript with input from all authors.

Additional information

Supplementary information is available in the online version of the paper. Reprints and permissions information is available online at www.nature.com/reprints. Correspondence and requests for materials should be addressed to T.K.B.

Competing financial interests

The authors declare no competing financial interests.